ITEP-TH-12/98
KANAZAWA-98-03
ZIF-MS-30/98

May 18, 1998, rev. June 9

Embedded Topological Defects in Hot Electroweak Theory: a Lattice Study

M. N. Chernodub[1,a], F. V. Gubarev[2,a], E.–M. Ilgenfritz[3,b] and A. Schiller[4,c,d]

[a] *ITEP, B.Cheremushkinskaya 25, Moscow, 117259, Russia*

[b] *Institute for Theoretical Physics, Kanazawa University, Kanazawa 920-1192, Japan*

[c] *Institut für Theoretische Physik, Universität Leipzig, D-04109 Leipzig, Germany*

[d] *Zentrum für interdisziplinäre Forschung, Universität Bielefeld, D-33615 Bielefeld, Germany*

ABSTRACT

We study the properties of Nambu monopoles and Z–vortices in the $3D$ lattice $SU(2)$ Higgs theory which represents the Standard Model at high temperature. We show that the densities of the Nambu monopoles and the Z–vortices are $O(1)$ in the symmetric phase and generically small in the Higgs phase. Near to the critical Higgs mass and in the vicinity of the phase transition the densities are no more negligible in the broken phase. The percolation probability of the Z–vortex lines is found as a new disorder parameter for this phase transition. We conclude that the transition to the symmetric phase is accompanied by Z–vortex condensation. Simulations comparing elementary and extended vortices and monopoles at different β_G values, aiming to show that the density of vortices and monopoles of fixed physical size might have a well-defined continuum limit, gives encouraging but so far inconclusive results.

[1]chernodub@vxitep.itep.ru
[2]Fedor.Gubarev@itep.ru
[3]ilgenfri@hep.s.kanazawa-u.ac.jp
[4]schiller@tph204.physik.uni-leipzig.de

1 Introduction

This paper is devoted to the study of topological properties of thermal states in the standard model of electroweak interactions. Although the standard model does not possess *topologically stable* monopole- and vortex-like structures, one can define so-called *embedded* topological defects [1, 2]: they are known under the names of Nambu monopoles [3] and Z–strings [3, 4]. We perform the investigation of the equilibrium thermodynamics of embedded topological defects in the framework of dimensional reduction which is expected to be reliable to describe the physics near to the transition temperatures (of a truly first order phase transition or a continuous crossover) for Higgs masses between 30 and 240 GeV.

Embedded topological defects play a crucial role in some electroweak baryogenesis scenarios. For example, one of the scenarios is based on the decay of an electroweak string network as the Universe cools down. According to this mechanism, long electroweak strings decay into smaller, twisted and linked string loops which carry non-zero baryon number. This could then explain the emergence of non-zero baryon number in the Universe [5]. Another example is the bound state picture of a sphaleron: a Nambu monopole–anti-monopole pair connected by a segment of Z–string [2, 6, 7] builds the unstable (saddle point) sphaleron field configuration [4, 8] in the broken phase. After the electroweak transition is completed, this type of electroweak configuration is the only transition state available between vacua of different Chern–Simons number. Thermal activation would allow to wash-out the baryon number asymmetry [9] and therefore has to be suppressed. In a recent paper [7] we have analyzed classical lattice sphalerons (as obtained and discussed in Ref. [10]) and have found evidence for the monopole–anti-monopole bound state picture of these configurations.

In the present publication, we apply the tools for detecting Nambu monopoles and Z–vortices developed in Ref. [7] in order to study numerically the formation of these defects in thermal equilibrium states of the electroweak theory. We measure the densities of Nambu monopoles and of Z–strings across the phase transition. In an attempt to substantiate the picture of Z–vortex condensation we also study the percolation probability of the Z–vortex line network near to the phase transition temperature. Recently, in a different context, in Ref. [11] convincing evidence has been provided that string percolation is a good disorder parameter for a phase transition in field theory.

Due to the smallness of the Weinberg angle θ_W the $U(1)$ component of the electroweak group $SU(2) \times U(1)$ can have only little effect on the properties of the embedded defects. Thus the dynamics of the topological defects can be studied restricting ourselves to the $SU(2)$ Higgs sector. The emerging effective $3D$ $SU(2)$ Higgs lattice model[a] allows to take into account effects of chiral fermions on physical parameters perturbatively [13, 14].

[a] Besides symmetric and Higgs phases, the lattice $SU(2)$ Higgs model in $4D$ has also the confinement phase which is located at sufficiently small β_G (which has, however, nothing to do with the electroweak theory in the continuum). One can show analytically that the transition between the symmetric and the confinement phase in that model is accompanied by Nambu monopole condensation [12]. This observation leads us to conjecture that topological defects may be relevant for the phase transitions also in the physically relevant region of the parameters of the $SU(2)$ Higgs model, which is studied here in its dimensionally reduced variant.

However, as in our study of the structure of the electroweak sphaleron one may expect that the influence of the standard model fermions on the embedded defects is small [9].

The structure of the paper is as follows. The effective three-dimensional model is shortly recalled in Section 2. In this Section we also give the lattice definitions of the embedded topological defects according to Ref. [7] and generalize them to cover the case of extended defects, too. In Section 3 we present the numerical results on the density of elementary (size a) monopoles and vortices and on the percolation probability of the corresponding Z–vortex lines. In Section 4 we describe a first step to extend this analysis to extended vortices and monopoles of equal physical size living on finer lattices in order to see whether the density discontinuities at the transition temperature possess a continuum limit. Section 5 contains a discussion of our results and conclusions.

2 Embedded Defects in Lattice $SU(2)$ Higgs Model

We study the lattice $3D$ $SU(2)$ Higgs model with the following action:

$$S = \beta_G \sum_p \Big(1 - \frac{1}{2}\mathrm{Tr}U_p\Big) - \beta_H \sum_{x,\mu} \frac{1}{2}\mathrm{Tr}(\Phi_x^+ U_{x,\mu}\Phi_{x+\hat{\mu}}) + \sum_x \Big(\rho_x^2 + \beta_R(\rho_x^2 - 1)^2\Big)\,, \quad (1)$$

where the summation is taken over plaquettes p, sites x and links $l = \{x, \mu\}$. The action contains three parameters: the gauge coupling β_G, the lattice Higgs self-coupling β_R and the hopping parameter β_H. The gauge fields are represented by unitary 2×2 link matrices $U_{x,\mu}$ and U_p denotes the $SU(2)$ plaquette matrix. The Higgs fields are parametrized as follows: $\Phi_x = \rho_x V_x$, where $\rho_x^2 = \frac{1}{2}\mathrm{Tr}(\Phi_x^+\Phi_x)$ is the Higgs modulus squared, and V_x an element of the group $SU(2)$. The lattice parameters are related to the continuum parameters of the $3D$ superrenormalizable $SU(2)$ Higgs model g_3, λ_3 and $m_3(\mu_3 = g_3^2)$ as given *e.g.* in [14]. As in [14] a parameter M_H^* is used (approximately equal to the zero temperature physical Higgs mass) which expresses the Higgs self-coupling as follows

$$\beta_R = \frac{\lambda_3}{g_3^2}\frac{\beta_H^2}{\beta_G} = \frac{1}{8}\Big(\frac{M_H^*}{80\ \mathrm{GeV}}\Big)^2 \frac{\beta_H^2}{\beta_G}\,. \quad (2)$$

The lattice coupling β_G and continuum coupling g_3^2 are related by

$$\beta_G = \frac{4}{a g_3^2}\,, \quad (3)$$

with a being the lattice spacing. We shall study the theory at different gauge couplings β_G in order to understand the qualitative behavior of the lattice embedded defects towards the continuum limit, *i.e.* when the lattice becomes fine enough to resolve the structure of defects which then have to be described as extended defects.

Let us first define elementary topological defects. The gauge invariant and quantized lattice definition of the Nambu monopole is closely related to the definition in the continuum theory [7]. First we define a composite adjoint unit vector field $n_x = n_x^a\,\sigma^a$, $n_x^a = -(\Phi_x^+\sigma^a\Phi_x)/(\Phi_x^+\Phi_x)$ with σ^a being the Pauli matrix. The field n_x plays a role similar to the direction of the adjoint Higgs field in the definition of the 't Hooft–Polyakov

monopole [15] in the Georgi–Glashow model. Then we define the gauge invariant flux plaquette $\bar{\theta}_p$:

$$\bar{\theta}_p(U,n) = \arg\Big(\mathrm{Tr}\left[(\mathbb{1}+n_x)V_{x,\mu}V_{x+\hat{\mu},\nu}V^+_{x+\hat{\nu},\mu}V^+_{x,\nu}\right]\Big)\,. \tag{4}$$

Here

$$V_{x,\mu}(U,n) = U_{x,\mu} + n_x U_{x,\mu} n_{x+\hat{\mu}} \tag{5}$$

has been used to define a particular projection of the gauge field. The sense of it becomes more transparent if we consider the unitary gauge where we have $\Phi_x = (0,\phi)^T$, $n^a_x \equiv \delta^{a3}$. In this gauge the phases $\theta^u_l = \arg U^{11}_l$ behave as a compact Abelian field with respect to the residual Abelian gauge transformations $\Omega^{abel}_x = e^{i\sigma_3\,\alpha_x}$, $\alpha_x \in [0,2\pi)$ which leave the unitary gauge condition intact. The Nambu monopoles are the topological defects in this Abelian field. The gauge invariant plaquette function (4) coincides with the standard Abelian plaquette formed out of the fields θ^u_l [7]. In this case, the Nambu monopole charges can be defined using the standard construction:

$$j_c = -\frac{1}{2\pi}\sum_{p\in\partial c}\bar{\theta}_p\,, \quad \bar{\theta}_p = (\theta_p - 2\pi m_p) \in [-\pi,\pi)\,. \tag{6}$$

In the gauge independent definition (4) the flux immediately gets values in the required interval $[-\pi,\pi)$ and is independent of the choice of the reference point x on the plaquette, due to the property $n_x V_{x,\mu} = V_{x,\mu} n_{x+\hat{\mu}}$.

The Z–string [4, 3] corresponds to the Abrikosov–Nielsen–Olesen vortex solution [16] embedded [1, 2] into the electroweak theory. The Z–vorticity number corresponding to the plaquette $p = \{x, \mu\nu\}$ is defined [7] similar to the construction of the Abelian vortices in an Abelian Higgs theory:

$$\sigma_p = \frac{1}{2\pi}\Big(\chi_p - \bar{\theta}_p\Big)\,, \tag{7}$$

where $\bar{\theta}_p$ has been given in eq. (4), and $\chi_{x,\mu\nu} = \chi_{x,\mu} + \chi_{x+\hat{\mu},\nu} - \chi_{x+\hat{\nu},\mu} - \chi_{x,\nu}$ is the plaquette variable formed out of Abelian links

$$\chi_{x,\mu} = \arg\left(\Phi^+_x V_{x,\mu}\Phi_{x+\hat{\mu}}\right)\,. \tag{8}$$

The Z–vortex is formed by the links $l = \{x,\rho\}$ of the dual lattice carrying non-vanishing vorticity ${}^*\sigma_l$. These links are dual to the plaquettes $p = \{x,\mu\nu\}$ with non-zero vortex number (7) and ${}^*\sigma_{x,\rho} = \varepsilon_{\rho\mu\nu}\sigma_{x,\mu\nu}/2$. One can show that Z–vortices begin and end on the Nambu (anti-) monopoles: $\sum_{\mu=1}^{3}({}^*\sigma_{x-\hat{\mu},\mu} - {}^*\sigma_{x,\mu}) = {}^*j_x$.

In order to understand the behavior of the embedded defects towards the continuum limit we have made measurements of densities of Nambu monopoles and Z–vortices *just of one definite physical size* which amounts to different multiples of a on different lattices. We follow the change from the broken to the symmetric phase at various gauge couplings, $\beta_G = 8, 16, 24$, *i.e.* with a lattice step size a getting smaller with increasing β_G. In principle, starting from a lattice simulated at various β_G, we could perform different factor k

real space renormalization group transformations of the gauge-Higgs field configurations in order to measure properties of defects of many different sizes ka objects in a manner described above. Instead of doing this, as a first step, we use here the notion of *extended* topological objects on the lattice as invented in Ref. [17]. An extended monopole (vortex) of physical size ka is defined on k^3 cubes (k^2 plaquettes, respectively).[b] The charge of monopoles $j_{c(k)}$ on bigger k^3 cubes $c(k)$ is constructed analogously to that of the elementary monopole, eq. (6), with the elementary 1×1 plaquettes in terms of $V_{x,\mu}$ replaced by $n \times n$ Wilson loops (extended plaquettes) denoted as $p(n)$.

First, the projected links $V_{x,\mu}(U, n)$ are defined as usual, then extended V-links

$$V^{(k)}_{X,\mu} = V_{X,\mu} V_{X+\hat{\mu},\mu} ... V_{X+(k-1)\hat{\mu},\mu} \tag{9}$$

are formed where X and $X + k\hat{\mu}$ denote points of the decimated lattice, which inherit the property $n_X V^{(k)}_{X,\mu} = V^{(k)}_{X,\mu} n_{X+k\hat{\mu}}$. Finally, the phase angles of length-k extended Higgs operators are defined as

$$\chi_{l(k)} = \chi^{(k)}_{X,\mu} = \arg\left(\Phi^+_X V^{(k)}_{X,\mu} \Phi_{X+k\hat{\mu}}\right) . \tag{10}$$

With the gauge invariant flux $\bar{\theta}_{p(k)}$ for the extended plaquettes defined analogously to (4) in terms of the extended V-links and with the extended plaquette angles $\chi_{p(k)}$ formed out of the extended links angles $\chi_{l(k)}$, the definitions of extended monopoles and vortices can be taken over from eqs. (6,7)

$$j_{c(k)} = -\frac{1}{2\pi} \sum_{p(k) \in \partial c(k)} \bar{\theta}_{p(k)} , \quad \sigma_{p(k)} = \frac{1}{2\pi}\left(\chi_{p(k)} - \bar{\theta}_{p(k)}\right) . \tag{11}$$

According to eq. (3) the physical size of the k^3 monopoles (or the k^2 vortices) in simulations done at $\beta_G = k\beta^{(0)}_G$ should be equal for all k. Roughly the same physical objects are hopefully described as elementary monopoles and vortices at $\beta^{(0)}_G$, too.

3 Scanning the Transition with Size a Defects

First, the formation of *elementary* Nambu monopoles and Z–vortices has been scanned across the electroweak phase transition. Monte Carlo simulations have been performed on cubic lattices of size $L^3 = 16^3$ at $\beta_G = 12$ for self-couplings λ_3 corresponding to $M^*_H = 30$ GeV and $M^*_H = 70$ GeV, see eq. (2). We varied the parameter β_H in order to locate the phase transition for given M^*_H and β_G. For the update we used the algorithms

[b] In the context of Abelian projections of pure Yang–Mills theory this construction is known as type-I extended monopoles [17]. So-called type-II monopoles have been defined in the same context. These are defined by adding the charges (currents) of elementary monopoles inside the extended cube $c(n)$, and type-II vortices can be constructed similarly. We have also tried this construction for our model and found that here this block spin transformation does not seem to lead to a well-defined continuum limit for extended defects contrary to the case of $SU(2)$ gluodynamics where the type-II Abelian monopoles behave according to the renormalization group [18]. In the limit $a \to 0$ the detection of size a topological defects with the definition given above is afflicted with increasing lattice artifacts.

described in Ref. [14] which combine Gaussian heat bath updates for the gauge and Higgs fields with several reflections for the fields to reduce the autocorrelations. Usually, the first order nature of the thermal transition is detected by a two-peak histogram in the volume average of ρ^2. The average over all Monte Carlo configurations $\langle\rho^2\rangle$ denotes the quadratic Higgs condensate, the discontinuity (for infinite volume) of which is related to the latent heat [14].

Here we are interested in the behavior of the lattice densities ρ_m of Nambu monopoles and ρ_v of Z–vortices and want to measure the percolation probability for the Z–vortex lines near to the phase transition. For each lattice configuration, the densities ρ_m and ρ_v are given by

$$\rho_m = \frac{1}{L^3}\sum_c |j_c|\,, \qquad \rho_v = \frac{1}{3L^3}\sum_p |\sigma_p|\,, \tag{12}$$

where c and p refers to elementary cubes and plaquettes. The monopole charge j_c and the Z–vorticity σ_p are defined in eq. (6) and eq. (7), respectively.

The percolation probability of the vortex lines ${}^*\sigma$ is defined with the help of the following two-point function [19]:

$$C(r) \;=\; \left(\sum_{x,y,i} \delta_{x\in{}^*\sigma^{(i)}}\,\delta_{y\in{}^*\sigma^{(i)}}\cdot\delta\Big(|x-y|-r\Big)\right)\cdot\left(\sum_{x,y}\delta\Big(|x-y|-r\Big)\right)^{-1}, \tag{13}$$

where the summation is taken over all points x, y of the dual lattice and over all connected clusters of vortex lines ${}^*\sigma^{(i)}$ (i labels distinct vortex clusters). The Euclidean distance between two points x and y is denoted as $|x-y|$. The notation $x \in {}^*\sigma^{(i)}$ means that the vortex world line cluster ${}^*\sigma^{(i)}$ passes through the point x.

Then the percolation probability is

$$C \;=\; \lim_{r\to\infty} C(r)\,. \tag{14}$$

This formula corresponds to the thermodynamical limit. In this case the function $C(r)$ can be fitted as $C(r) = C + C_0 r^{-\alpha} e^{-mr}$, with C, C_0, α and m being fitting parameters. In our finite volume we find numerically that $m \sim a^{-1}$ in the studied region of the phase diagram. Therefore we can be sure that finite size corrections to C are exponentially suppressed. If C does not vanish, *i.e.* if two infinitely separated points with non-zero probability belong to the same connected cluster of vortex lines, the vacuum is populated by *infinitely long* vortex lines. In other words, an effective theory of these vortices would have an action smaller than the entropy per length of the vortex trajectory. This case implies the existence of a vortex condensate. If C turns to zero the vortex condensate vanishes [19].

In Figure 1(a) we show the ensemble averages of densities, $\langle\rho_m\rangle$ of Nambu monopoles and $\langle\rho_v\rangle$ of Z–vortices *vs.* hopping parameter β_H for Higgs mass $M_H^* = 30$ GeV at gauge coupling $\beta_G = 12$. At this Higgs mass the phase transition is of strongly first order [20]. It is seen that the averages of both densities are $O(1)$ in the symmetric phase and they sharply drop at the phase transition to zero densities in the Higgs phase. In Figure 1(b) the percolation probability C for the same parameters is shown to have a

small discontinuity at the transition. Deeper into the symmetric phase the condensate (percolation probability) grows while it is strictly vanishing in the broken phase.

For comparison, Figure 2(a) presents the Monte Carlo averages $\langle \rho_m \rangle$ and $\langle \rho_v \rangle$ for the Higgs mass $M_H^* = 70$ GeV at $\beta_G = 12$. This Higgs mass parameter is very near to the critical Higgs mass. Now, the average densities of Nambu monopoles and Z–strings do not vanish immediately after the phase transition towards the broken phase: both densities are non-zero at temperatures $T \lesssim T_c$. Still, the corresponding vortices *do not percolate*. The percolation probability C for the Z–vortex trajectories behaves as a disorder parameter also in *this* case when the high-temperature electroweak phase transition is already very weakly first order [14]. It turns to zero exactly at β_{Hc} as can be seen in Figure 2(b) but a continuous behavior cannot be excluded from these data.

At the larger Higgs mass $M_H^* = 70$ GeV, just for the value of the gauge coupling $\beta_G = 12$ studied before, we have also tried to understand how the infinite volume limit is approached. We show in Fig. 3(a) and Fig. 3(b) histograms of the Nambu monopole density ρ_m and of the Z–vortices ρ_v, respectively, for lattice sizes 16^3, 24^3, 32^3 and 40^3. Even near to the end of the first order phase transition, we see that not exceedingly large lattices are necessary to see the two-state signal in the densities and to measure the (finite volume) discontinuity of the densities, such that its infinite volume limit can be obtained. In the present state of our analysis we cannot yet present corresponding histograms of the percolation probability which would allow to tell whether the weakly first order phase transition is still accompanied by a discontinuous change of the vortex condensate. Independent of this, one may say that an infinite percolating network is breaking into finite pieces at the transition temperature while the correlation length stays finite.

4 Is There a Continuum Limit ?

In Ref. [21] lattice vortices have been studied in the non-compact version of the $3D$ Abelian Higgs model. The $3D$ Abelian Higgs model has become a model system for many phase transitions, covering the electroweak and the QCD deconfinement transition, superconductivity as well as cosmic strings. From their attempt to define a well-defined continuum limit of the vortex density two lessons can be drawn. First, the lattice density might be afflicted by regularization artifacts such that, generally speaking, discontinuities at the phase transition are physically better defined. Second, one should carefully associate the density of defects with (various) physical scales and try to find the continuum limit of these. At least at the strongly first order phase transition at small Higgs mass the first problem seems to be not to so severe. But in order to get a physically well-defined vortex and monopole density, the extrapolation to the continuum limit requires the measurement of more and more extended defects on finer and finer lattices.

For a preliminary exploration we have concentrated on the case of Higgs mass $M_H^* = 30$ GeV where the phase transition is of strongly first order. At this Higgs mass the finite volume effects are numerically small and therefore we felt safe to study only one lattice size, 16^3, at various β_G. For the coarsest lattice we have chosen $\beta_G = \beta_G^{(0)} = 8$. Just to be specific, we have chosen the lattice spacing corresponding to this gauge coupling as the

size of topological objects to be examined for a reasonable continuum limit. Now we have measured at $\beta_G = k\beta_G^{(0)}$ (for $k = 2, 3$) histograms for the densities of extended monopoles and vortices of a size (in lattice units) of k^3 and k^2, respectively. The measurements were done near to the pseudocritical β_H for the appropriate gauge coupling at this lattice size.

The distributions of Nambu monopole and Z–vortex densities (for objects of corresponding *physical* size) are shown in Fig. 4(a) and (b), respectively. These (normalized) distributions of extended defects have the same two-peak structure as elementary ones. With decreasing inverse gauge coupling $1/\beta_G$ the metastability becomes weaker if the density of the defects is measured. At the smallest $\beta_G = 8$, for instance, where we looked for size a defects, we could not observe tunnelling between the two phases within 10000 iterations following hot/cold starts. In the Figures, for that β_G, the histograms corresponding to the Higgs phase are omitted since only the bin at zero density is populated. The peaks corresponding to the symmetric phase shift considerably from elementary objects at $\beta_G = 8$ to size-2 objects at $\beta_G = 16$, but only slightly from this measurement to size-3 objects at $\beta_G = 24$.

We have also checked the percolation of extended vortices. At $\beta_G = 16$ on a 16^3 lattice we have found $\beta_{Hc} = 0.3391$. Considering all possible $k = 2$ decimations, we have now analyzed networks of $k = 2$ vortices on this lattice with respect to percolation. There are 2^3 different $k = 2$ vortex configurations per gauge-Higgs configuration which have been obtained at $\beta_H = 0.3390$ and $\beta_H = 0.3392$. At $\beta_H = 0.3390$ we have found a non-zero condensate also for these extended objects, whereas at $\beta_H = 0.3392$ the condensate is strictly vanishing. We have to admit that this result has been obtained on a very small lattice. Nevertheless it is indicative for extended vortices percolating at the same temperature.

Similar measurements have to be repeated for defects of different scale on lattices with different lattice spacings and with bigger, physically comparable volumes before an understanding of the topological mechanism can be achieved. Notice that the above results were obtained concentrating, somewhat arbitrarily, on topological objects with smallest possible size that could be analysed on the coarsest, $\beta_G = 8$ lattice. Obviously, the next task is to study non-elementary topological objects already on the coarsest lattice. This endeavour requires much more computer power in view of the complementing measurements that have to be done on finer lattices covering the same volume. Since our studies already indicate that (within our lattice construction) Nambu monopoles and Z–vortices as topological excitations of definite physical size become more and more well-defined in the continuum limit, it seems to be preferable to dispense with the elementary objects completely.

The observed, more well-defined behavior is related to the way how the fundamental Higgs field is turned into an auxiliary composite field used to project out the Abelian fluxes. It seems, that their densities possess a sensible continuum limit which can be measured by our lattice prescription. In contrast to this, elementary monopoles and vortices are still far from the continuum limit for defects of corresponding size. A similar problem is well-known for instantons in $4D$ lattice gauge theory.

As indicated above, there is another possibility to define extended defects of any size for a sufficiently fine lattice to start with. This requires to perform block spin transformations of Higgs and gauge fields which give a consistent description of the phase transition if seen

from different length scales. In Ref. [22] two of us have indicated a practical way how to do this.

5 Discussion and Conclusions

We have studied numerically the properties of Nambu monopoles and Z–vortices which appear as embedded defects in the Standard model at high temperatures. Our results are obtained in the $3D$ lattice formulation of the $SU(2)$ Higgs sector. We have shown that these defects are dense in the symmetric phase and that they exist as a more or less dilute gas in the Higgs phase. Moreover, the percolation probability of the Z–vortex trajectories has been shown to be *the* disorder parameter for the hot electroweak phase. The Z–strings are condensed in the symmetric phase, and the condensate vanishes in the broken phase. This result has been obtained for the Higgs mass $M_H^* = 30$ GeV at which the phase transition is of strongly first order. The same is found to be true for the Higgs mass $M_H^* = 70$ GeV (weakly first order phase transition) where the density of monopoles and vortices is clearly discriminating the phases. Note that in this case at the phase transition the densities in the broken phase are *not less* than 50 % of the corresponding ones in the symmetric phase[c].

Comparing the densities of the embedded defects of corresponding physical size at various values of the gauge coupling β_G gives a first hint that the densities of extended Nambu monopoles and Z–strings as defined in this paper might possess a well-defined continuum limit. Further studies are necessary to understand the dynamics of defects and the spatial structure of vortices of different physical size near to the transition and in the high temperature phase.

The approach of this investigation may be extended to lattice $SU(2)$ Higgs model in $D = 3 + 1$. In this case the Z–vortex world trajectories are sweeping out two dimensional world surfaces which are open on the monopole world lines. According to analytical estimates [24] the Z–vortices form a dense network of long strings at temperatures above a temperature which has been termed Hagedorn temperature T_H in analogy to the dual resonance theory of hadronic strings with its exponentially rising mass spectrum. One would expect this temperature to be of the order of the critical temperature or slightly smaller, $T_H \lesssim T_c$. Below T_H the network decays into small loops eventually producing non-zero baryon number [5]. We hope to be able to substantiate this picture by $4D$ lattice studies in near future.

Acknowledgements

M. N. Ch. and F. V. G. are grateful to M. I. Polikarpov and K. Selivanov for interesting discussions, E.-M. I. thanks T. Suzuki for useful remarks.

[c]Even after the phase transition has ceased to exist at larger Higgs masses, preliminary results at $M_H^* = 100$ GeV show that the condensate of vortices turns to zero at the crossover transition temperature [23].

M. N. Ch. acknowledges the kind hospitality of the Institute of Physics of Humboldt University (Berlin) where this project has been initiated. M. N. Ch. and F. V. G. were partially supported by the grants INTAS-96-370, INTAS-RFBR-95-0681, RFBR-96-02-17230a and RFBR-96-15-96740.

References

[1] T. Vachaspati and M. Barriola, *Phys. Rev. Lett.* **69** (1992) 1867.

[2] M. Barriola, T. Vachaspati and M. Bucher, *Phys. Rev.* **D50** (1994) 2819.

[3] Y. Nambu, *Nucl. Phys.* **B130** (1977) 505.

[4] N. S. Manton, *Phys. Rev.* **D28** (1983) 2019.

[5] T. Vachaspati, *Phys. Rev. Lett.* **73** (1994) 373.

[6] M. Hindmarsh and M. James, *Phys. Rev.* **D49** (1994) 6109; M. Hindmarsh, in *Electroweak Physics and the Early Universe*, J. C. Romão and F. Freire (Eds.), Plenum, New York, 1995, p. 195, `hep-ph/9408241`.

[7] M. N. Chernodub, F. V. Gubarev and E.–M. Ilgenfritz, *Phys. Lett.* **B424** (1998) 106.

[8] R. F. Dashen, B. Hasslacher and A. Neveu, *Phys. Rev.* **D10** (1974) 4138; F. R. Klinkhamer and N. S. Manton, *Phys. Rev.* **D30** (1984) 2212.

[9] V. A. Rubakov and M. E. Shaposhnikov, *Usp. Fiz. Nauk* **166**(1996) 493 (*Phys. Usp.* **39** (1996) 461).

[10] M. Garcia Perez and P. van Baal, *Nucl. Phys.* **B429** (1994) 451; *Nucl. Phys.* **B468** (1996) 277.

[11] N. D. Antunes, L. M. A. Bettencourt and M. Hindmarsh, *Phys. Rev. Lett.* **80** (1998) 908.

[12] M. N. Chernodub, *JETP Lett.*, **66** (1997) 605.

[13] K. Kajantie *et al.*, *Nucl. Phys.* **B466** (1996) 189.

[14] M. Gürtler *et al.*, *Nucl. Phys.* **B483** 383 (1997); M. Gürtler, E.–M. Ilgenfritz and A. Schiller, *Phys. Rev.* **D56** (1997) 3888.

[15] G. 't Hooft, *Nucl. Phys.* **B79** (1974) 276; A. M. Polyakov, *JETP Lett.* **20** (1974) 194.

[16] A. A. Abrikosov, *Sov. Phys. JETP* **32** (1957) 1442; H. B. Nielsen and P. Olesen, *Nucl. Phys.* **B61** (1973) 45.

[17] T. L. Ivanenko, A. V. Pochinskii and M. I. Polikarpov, *Phys. Lett.* **B252** (1990) 631.

[18] H. Shiba and T. Suzuki, *Phys. Lett.* **B351** (1995) 519; T. Suzuki *et al.*, *Nucl. Phys.* **B** Proc. Suppl. **53** (1997) 531.

[19] A. V. Pochinsky, M. I. Polikarpov and B. N. Yurchenko, *Phys. Lett.* **A154** (1991) 194; A. Hulsebos, `hep-lat/9406016`; *Nucl. Phys.* **B** *(Proc. Suppl.)* **34** (1994) 695.

[20] E.–M. Ilgenfritz *et al.*, *Phys. Lett.* **B356** (1995) 561.

[21] K. Kajantie *et al.*, `hep-ph/9803367`, to appear in *Phys. Lett.* **B**.

[22] E.–M. Ilgenfritz and A. Schiller, *Int. J. Mod. Phys.* **C5** (1994) 373.

[23] M. N. Chernodub, F. V. Gubarev, E.–M. Ilgenfritz and A. Schiller, in progress.

[24] T. Vachaspati, in *Electroweak Physics and the Early Universe*, J. C. Romão and F. Freire (Eds.), Plenum, New York, 1995, p. 171, `hep-ph/9405286`.

Figures

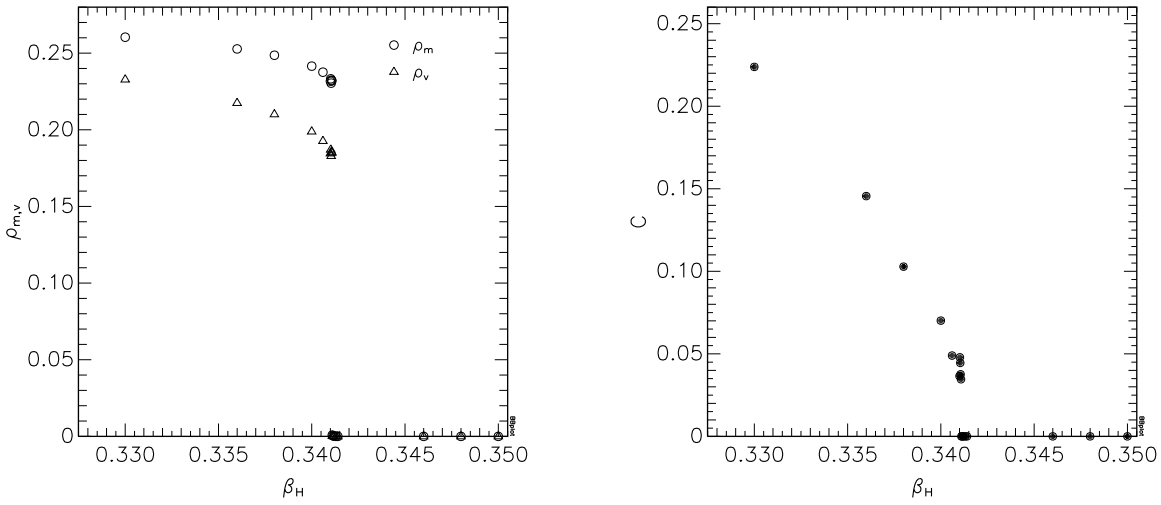

(a) (b)

Figure 1: (a) Density of Nambu monopoles ρ_m and of Z–vortices ρ_v *vs.* hopping parameter β_H for Higgs mass $M_H^* = 30$ GeV at gauge coupling $\beta_G = 12$; (b) Percolation probability C of Z–vortex trajectories for the same parameters; the critical hopping parameter is $\beta_{Hc} \approx 0.3411$.

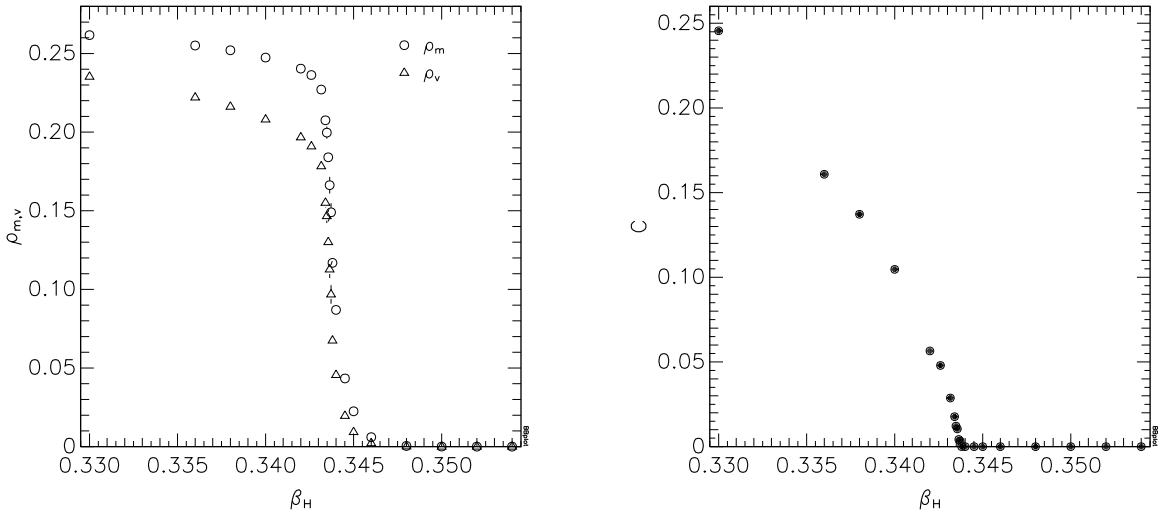

(a) (b)

Figure 2: Same as in Figure 1 for $M_H^* = 70$ GeV; the critical hopping parameter is $\beta_{Hc} \approx 0.34355$.

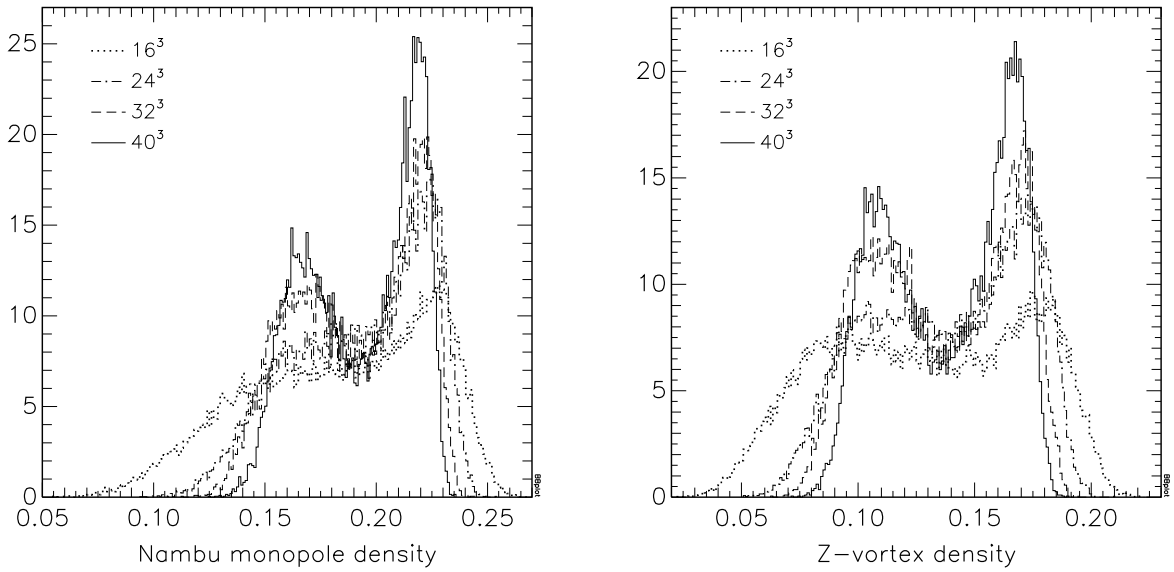

(a) (b)

Figure 3: Density distributions of Nambu monopoles (a) and of Z–vortices (b) of elementary size at pseudocriticality for different lattice sizes, $M_H^* = 70$ GeV and $\beta_G = 12$.

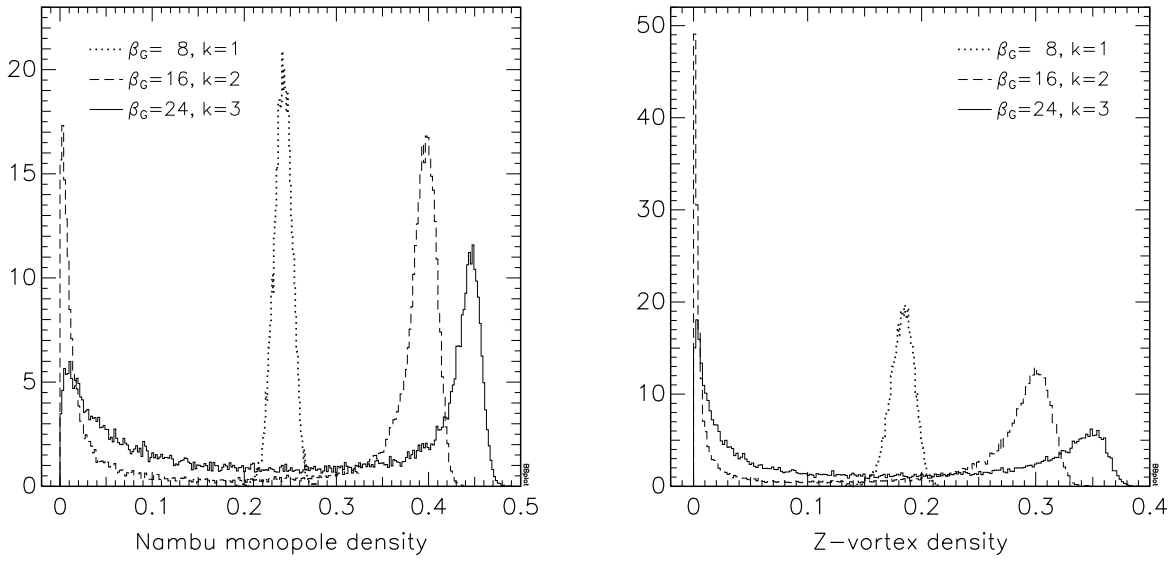

(a) (b)

Figure 4: Density distributions of Nambu monopoles (a) and of Z–vortices (b) of fixed physical size at pseudocriticality for different gauge couplings, Higgs mass $M_H^* = 30$ GeV and 16^3 lattice.